Characterization of the two conformations adopted by the T3SS inner-membrane protein PrgK.

Supplementary information

Julien R. C. Bergeron[1,2,5], Jacob A. Brockerman[1], Marija Vuckovic[1], Wanyin Deng[4], Mark Okon[1,3], Brett B. Finlay[1,4], Lawrence P. McIntosh[1,3,4]*, Natalie C.J. Strynadka[1,2]*.

[1] Department of Biochemistry and Molecular Biology, University of British Columbia, Vancouver, BC, Canada V6T 1Z3

[2] Centre for Blood Research, University of British Columbia, Vancouver, BC, Canada V6T 1Z3

[3] Department of Chemistry, University of British Columbia, Vancouver, BC, Canada V6T 1Z1

[4] Michael Smith Laboratories, University of British Columbia, Vancouver, BC, Canada V6T 1Z4

[5] Current address: Department of Molecular Biology and Biotechnology, The University of Sheffield, Sheffield, UK

* To whom correspondence should be addressed: ncjs@mail.ubc.ca and mcintosh@chem.ubc.ca

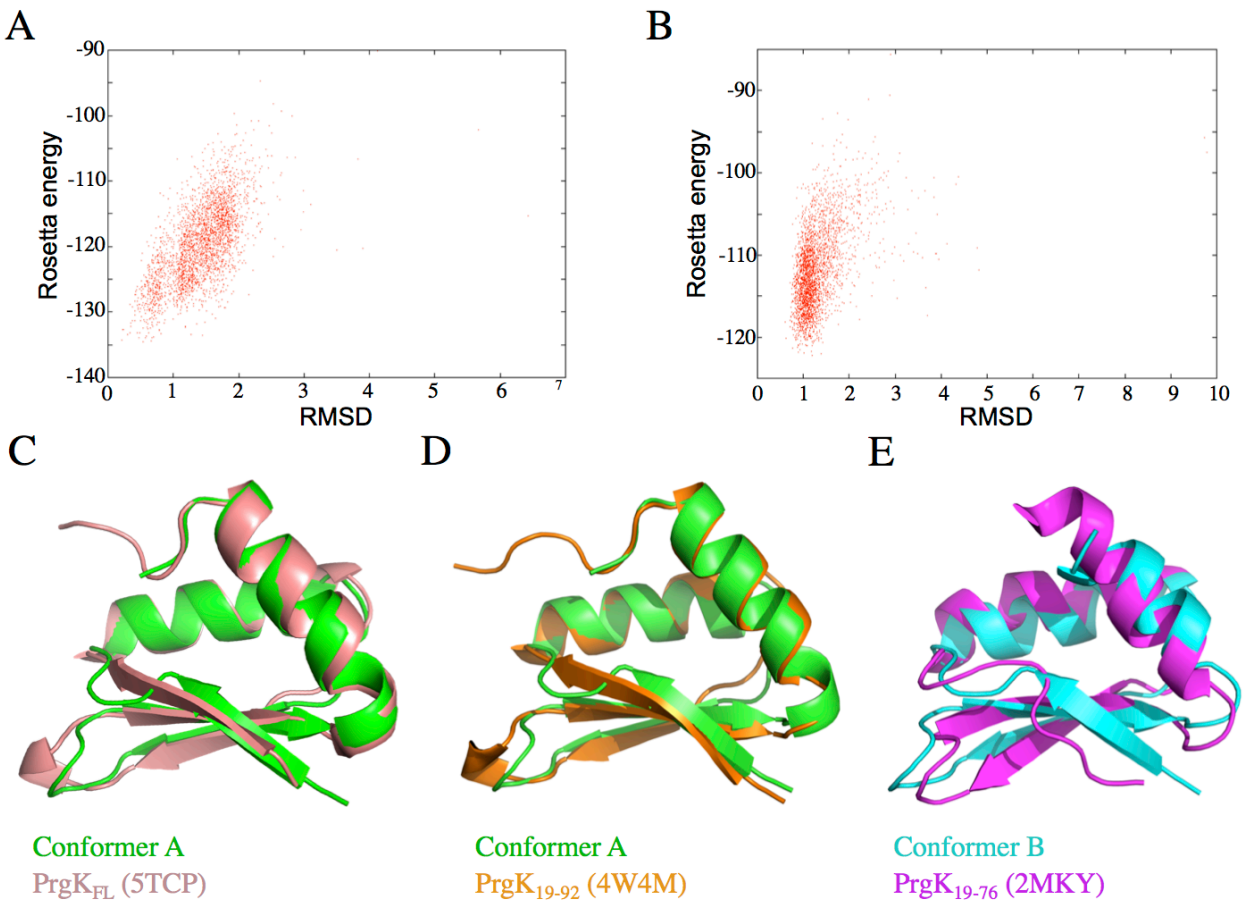

Figure S1: Comparison of the various PrgK D1 structures.

The Rosetta energies for the two conformers are plotted in (A) and (B) respectively, relative to the RMSD with the lowest-energy model. Both structural ensembles correspond to well converging, low energy models. Disordered regions were truncated according to the Lange method[40], such that only residues 19-78 were modeled for conformer A, and residues 19-74 for conformer B. (C) A portion of the structure of full length PrgK, from the basal body cryo-EM map (PDB ID 5CTP, salmon) and (D) the crystal structure of PrgK$_{19-92}$ (PDB ID 4W4M, orange) overlaid on the CS-Rosetta structural model of conformer A (green) determined in this study. (E) The solution structure of PrgK$_{19-76}$ (i.e. D1 only), determined using NOE-derived distance restraints (PDB ID 2MKY, magenta), overlaid on the CS-Rosetta structural model of conformer B (cyan).

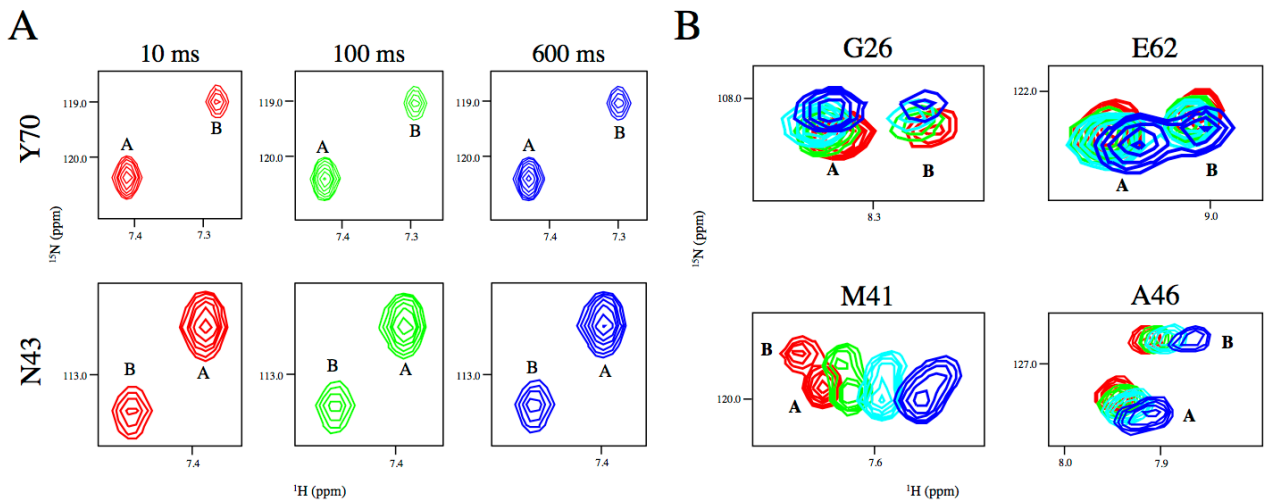

Figure S2: The two alternative conformations are in very slow exchange.

(A) Selected regions of the ^{15}N-EXSY spectra of PrgK$_{19\text{-}92}$, recorded with an 850 MHz NMR spectrometer at 3 different mixing times. Shown are residues where the peaks yielded by the two conformers have clearly separated chemical shifts in both ^{1}H and ^{15}N dimensions. Even at the longest mixing time (600 msec), no exchange cross-peaks are detected. This is indicatives that the exchange between the two populations is slow with $k_{ex} \lesssim 1\ s^{-1}$. (B) Selected regions of the overlaid ^{15}N-HSQC spectra of PrgK$_{19\text{-}92}$, acquired at different temperatures (10 °C in blue, 20 °C in cyan, 30 °C in green and 40 °C in red). Spectra were collected at 8 different temperatures, from 10 to 45°C in 5 °C increments, but only 4 representative spectra are shown for clarity. Although the chemical shifts of many peaks are affected by the temperature change, the relative intensity ratios of peak corresponding the two populations are not visibly affected.

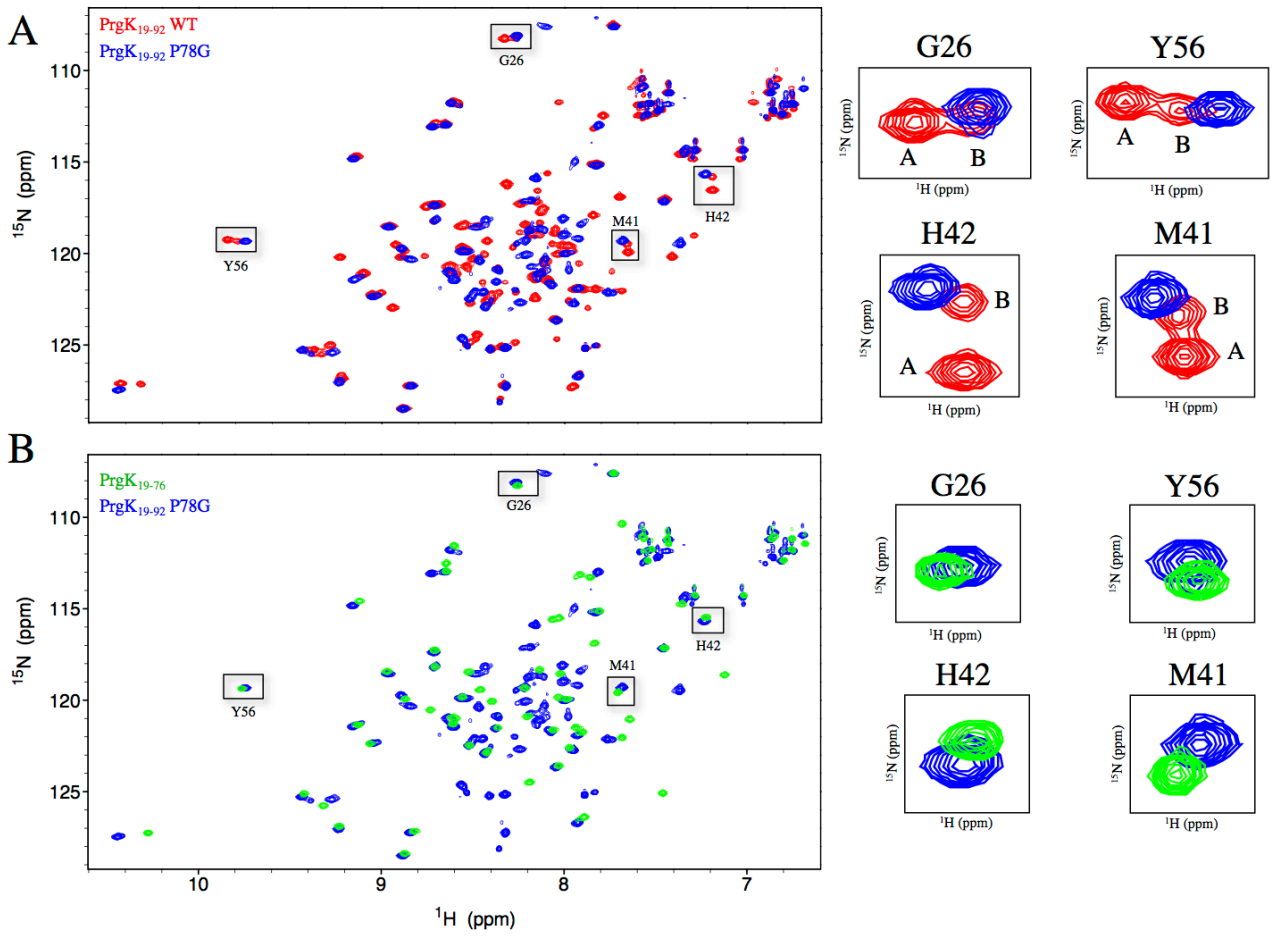

Figure S3: The conformational equilibrium of PrgK is dependent on Pro78.

The ^{15}N-HSQC spectrum of PrgK$_{19\text{-}92}$ with the P78G mutation (blue), overlaid on that of the WT protein (A, red) or the PrgK$_{19\text{-}76}$ construct (B, green). Expanded regions for selected peaks are shown on the right, with A and B assignments indicated. The amide $^{1}H^{N}$-^{15}N signals of the P78G mutant overlay well with those corresponding to conformer B in the WT protein, and with those yielded by the PrgK$_{19\text{-}76}$ construct, indicating that this mutation prevents the formation of conformer A with the linker-bound conformation. However, in the spectrum of PrgK$_{19\text{-}92}$ P78G, the signal from the indole $^{1}H^{\varepsilon 1}$-$^{15}N^{\varepsilon 1}$ of Trp71 appears to overlay more closely with that of conformer A than conformer B. This may reflect additional uncharacterized interactions of Trp71 with linker residues in the mutated PrgK$_{19\text{-}92}$ that are not possible in the wild type PrgK$_{19\text{-}92}$ or the truncated PrgK$_{19\text{-}76}$.

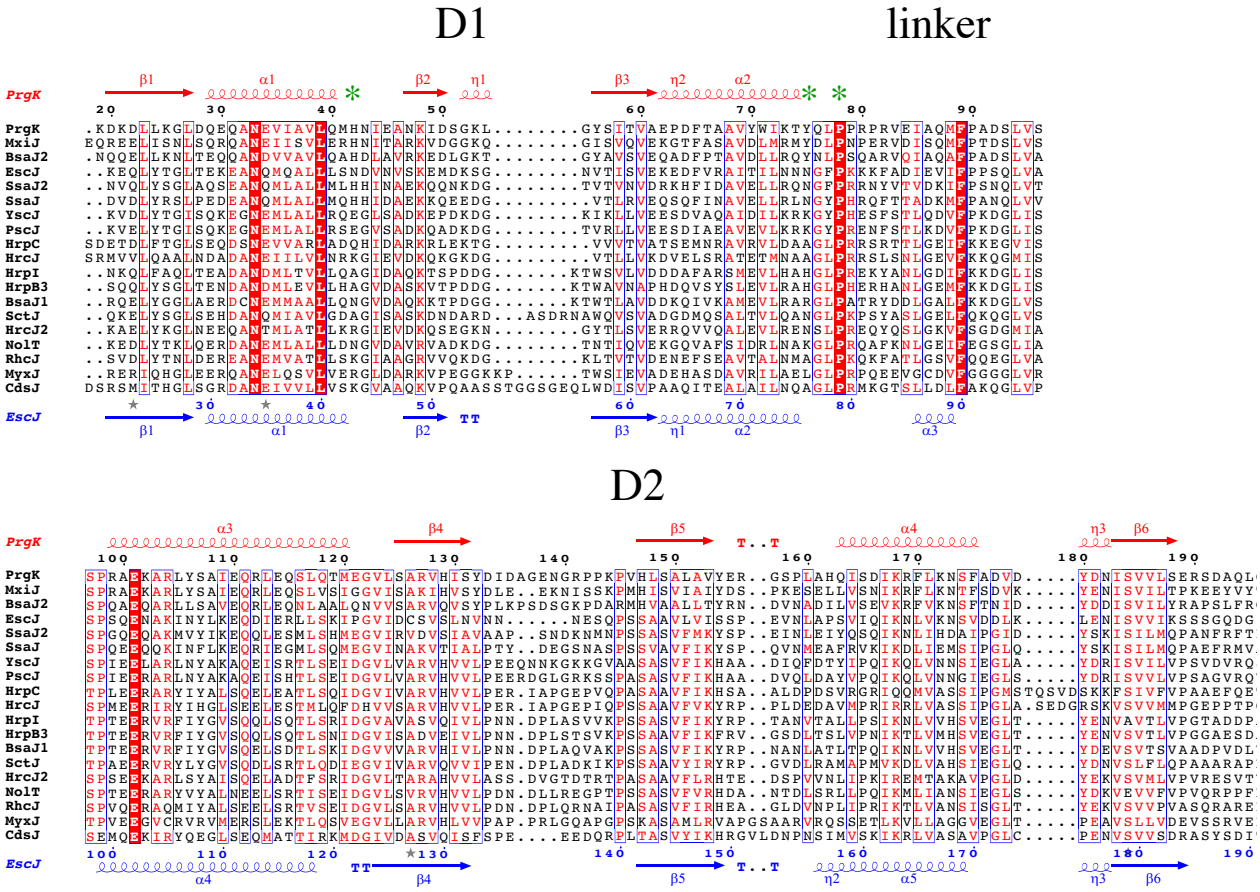

Figure S4: Multiple sequence alignment of PrgK homologues.

PrgK homologue sequences from the major T3SS families (*S. typhimurium* SPI-1 PrgK, *Shigella flexneri* MxiJ, *Burkholderia pseudomallei* T3SS3 BsaJ2, *E. coli* O127:H6 (EPEC) LEE EscJ, *Candidatus Hamiltonella* SsaJ2, *S. typhimurium* SPI-2 SsaJ, *Y. enterocolitica* YscJ, *P. aeruginosa* PscP, *P. syringae* HrpC, *Herbaspirillum seropedicae* HrcJ, *Ralstonia solanacearum* HrpI, *Xanthomonas axonopodis* HrpB3, *Burkholderia pseudomallei* T3SS1 BsaJ1, *Burkholderia pseudomallei* T3SS2 SctJ, *Desulfovibrio vulgaris* HrcJ2, *Rhizobium etli* NolT, *Sinorhizobium fredii* RhcJ, *Myxococcus fulvus* MyxJ and *Chlamydia trachomatis* CdsJ) were aligned with ClustalW, and the alignment figure was generated with ESPript. Conserved residues are in red boxes, similar residues are in red font, the secondary structure of PrgK (PDB ID 4W4M) is at the top in red, and that of EscJ (PDB ID 1YJ7) is at the bottom in blue. Key residues discussed in this study are indicated with green asterisks.

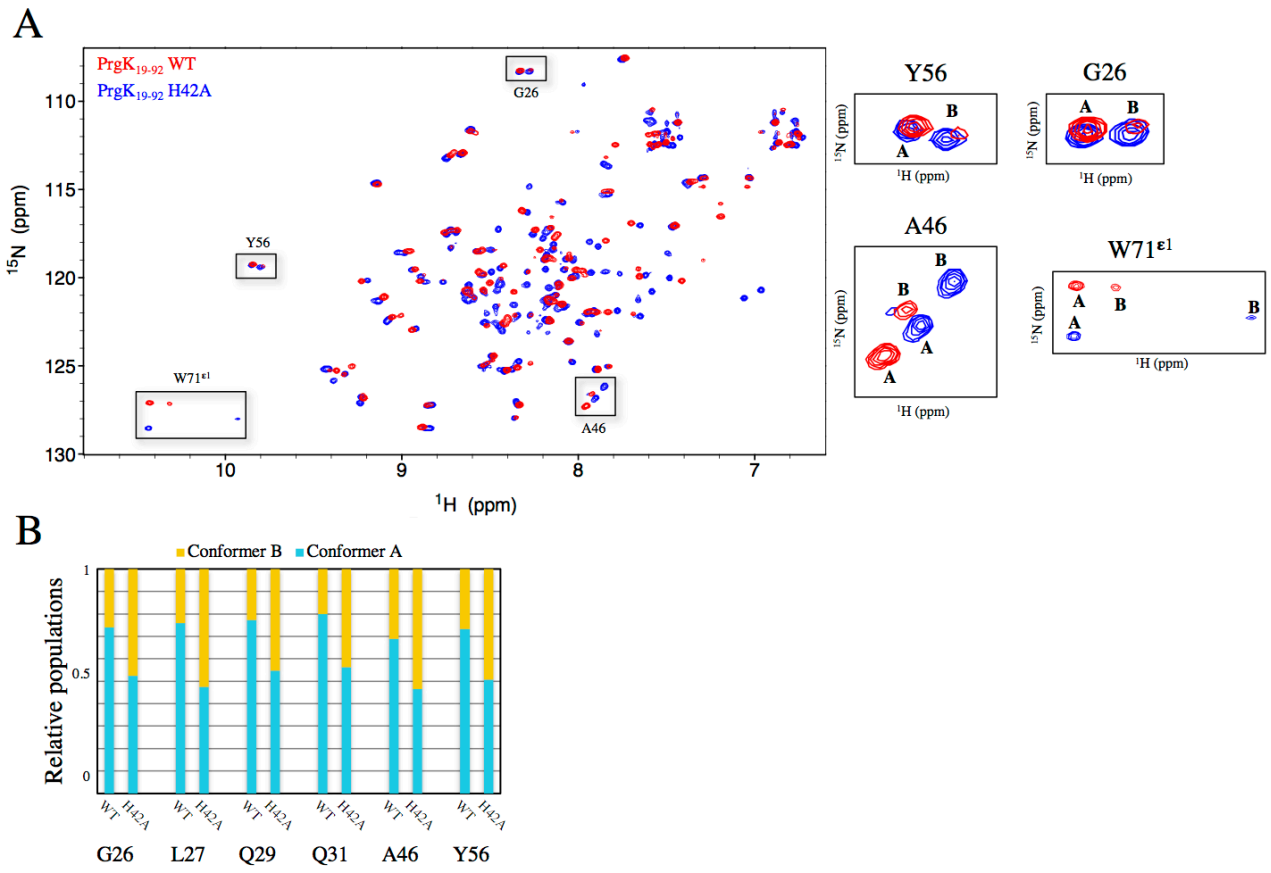

Fig.S5: Comparison of the PrgK$_{19\text{-}92}$ WT and H42A HSQC spectra

Figure S5: Comparison of the PrgK$_{19\text{-}92}$ WT and H42A spectra.

(A) The ^{15}N-HSQC spectrum of PrgK$_{19\text{-}92}$ H42A (blue), overlaid on that of the WT protein (red), both acquired at pH 7.0. Selected regions of the spectrum, with assigned peaks labeled, are shown on the right. Many amide signals are perturbed in the mutant protein. This suggests that the H42A mutation leads to an overall change in the protein conformation, not limited to the D1-linker interaction. Nonetheless, many peaks can still be readily identified, indicating that the overall structure of the protein is conserved. (B) Ratios of relative $^{1}H^{N}$-^{15}N peak intensities for amides in the WT and H42A proteins at pH 7. The average population of conformer A is ~ 0.5 for the H42A mutant, and 0.74 for the WT protein [(Fig. 4(B)]. However, the signal from the Trp71 indole $^{1}H^{\varepsilon 1}$-$^{15}N^{\varepsilon 1}$ in conformer B appears anomalously weak; reasons for this are not clear, but indicate faster relaxation than in conformer A.

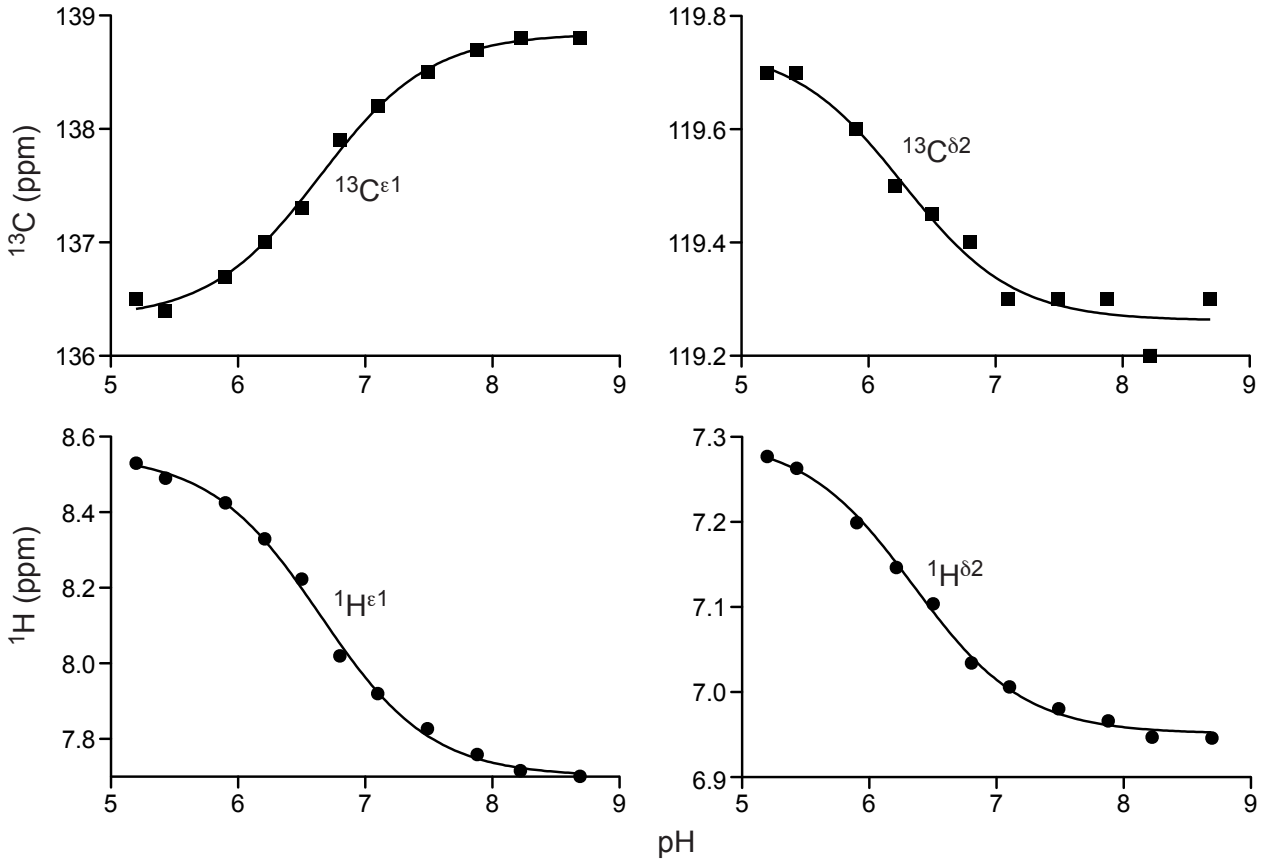

Figure S6: pK_a determination for the non-native N-terminal histidine of the PrgK$_{19\text{-}91}$ construct.

Averaging the individual fits of the pH-dependent chemical shifts of four nuclei in the N-terminal histidine of PrgK$_{19\text{-}91}$ (spectra not shown) to the equation for a single acid-base equilibrium yields an unperturbed pK_a value of 6.5 ± 0.2. Also, the small upfield shift of the $^{13}C^{\delta 2}$ signal (and an approximate 4 ppm downfield shift of the $^{13}C^{\gamma}$ signal; not shown) upon deprotonation is indicative of an equilibrium between major $N^{\varepsilon 2}H$ and minor $N^{\delta 1}H$ tautomers. Similar pK_a values and pH-dependent chemical shift changes seen with model histidine-containing peptides.